Supplemental Information for

Human influence on winter precipitation trends (1921-2015) over North America and Eurasia revealed by dynamical adjustment

Ruixia Guo[1,2], Clara Deser[1,*], Laurent Terray[3] and Flavio Lehner[1]

[1] Climate and Global Dynamics Laboratory, National Center for Atmospheric Research, Boulder, USA

[2] Key Laboratory for Semi-arid Climate Change of the Ministry of Education, College of Atmospheric Sciences, Lanzhou University, Lanzhou, China

[3] Climate, Environment, Coupling and Uncertainties group, Université de Toulouse, CERFACS/CNRS, Toulouse, France

* *Corresponding author*: Clara Deser (cdeser@ucar.edu)

Contents: Figures S1-S7.

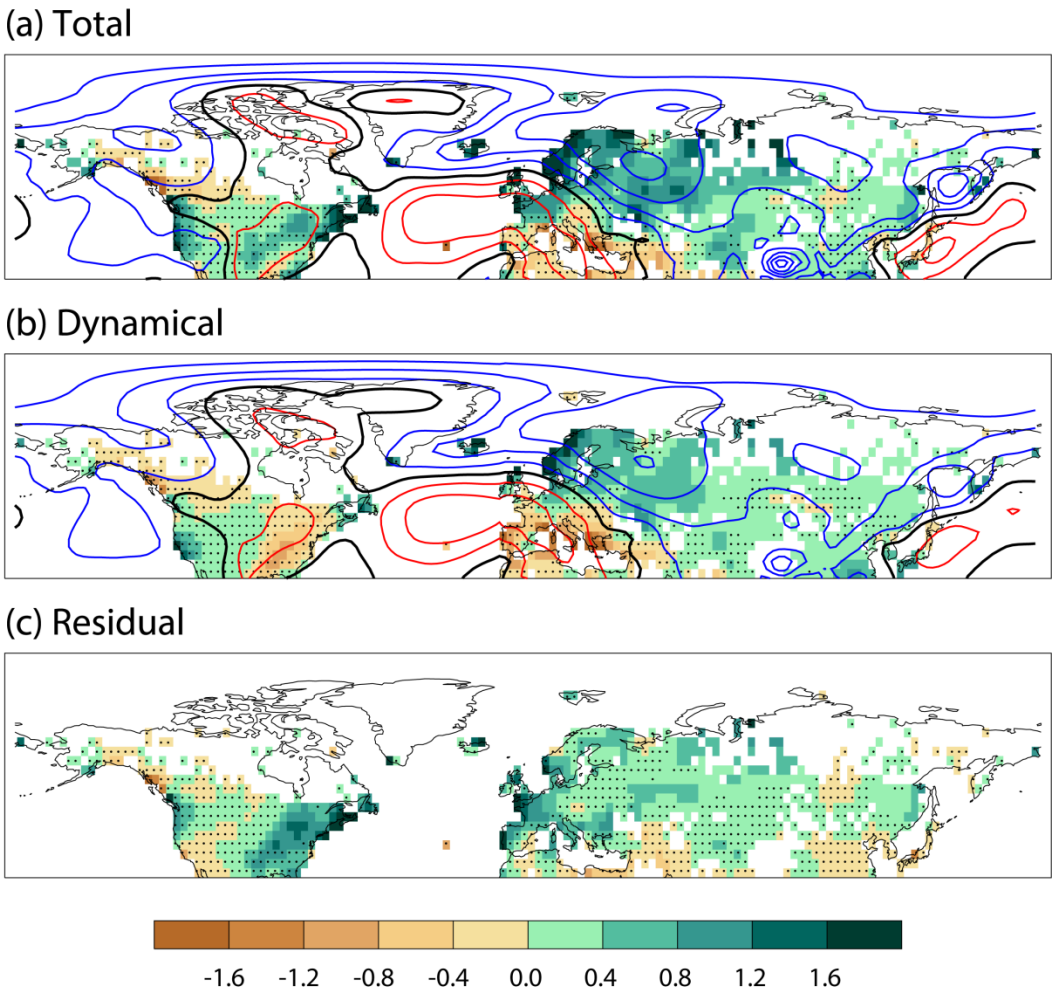

Figure S1. As in Figure 1 in the main text, but based on CRU precipitation. (a) Observed winter (November-March) precipitation (color shading; mm/month per decade) and SLP (contours, hPa per decade) trends (1921-2015). (b) Dynamical contribution to (a). (c) Thermodynamic residual (a minus b). Ensemble-mean precipitation and SLP trends from (d) CMIP5 and (e) CESM1. In all panels, the SLP contour interval is 0.1 hPa per decade, with positive (negative) values in red (blue) and the zero contour in black (suppressed for clarity in panel c). Stippled regions denote precipitation trends that are insignificant at the 90% confidence level based on a two-sided Student-t test.

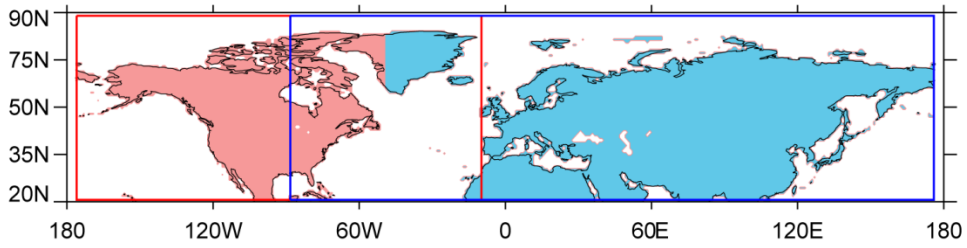

Figure S2. Domains used in the dynamical adjustment procedure. Red and blue boxes denote the SLP domains used to dynamically adjust precipitation over North America (red shading) and Eurasia (blue shading), respectively.

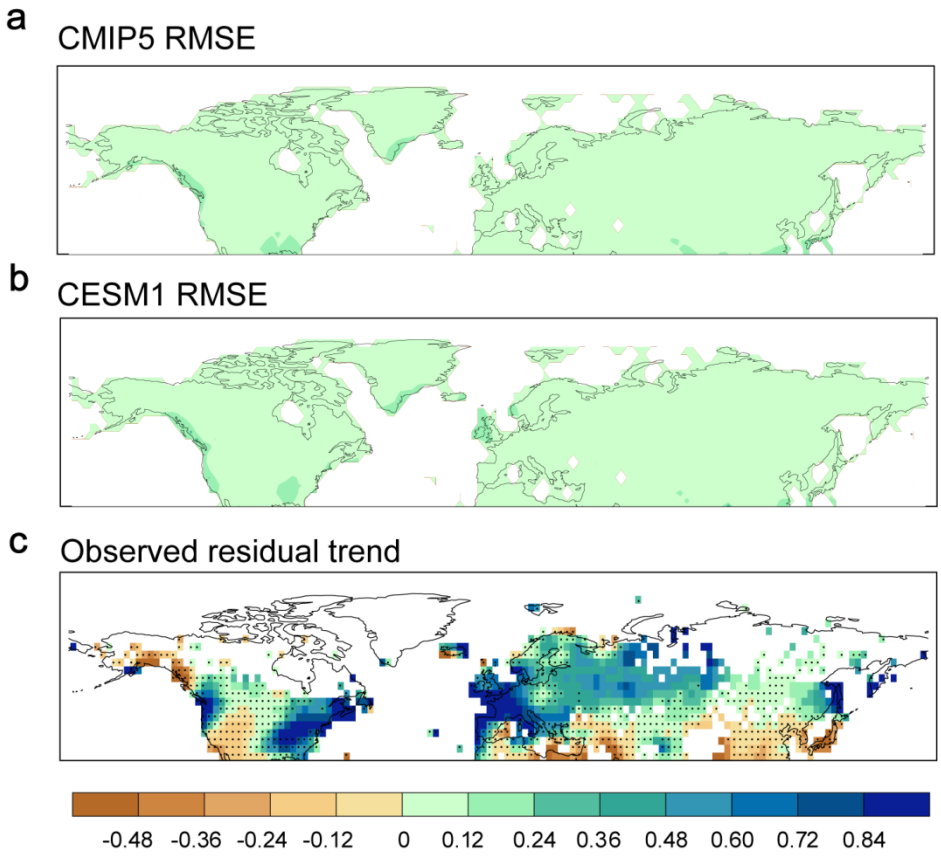

Figure S3. Comparison of the magnitude of the root-mean-squared-error (RMSE) of the dynamical adjustment methodology and the observed thermodynamic residual winter (November-March) precipitation trend (1921-2015; mm mo^{-1} per decade). Here, the RMSE is computed from the differences between the dynamically-adjusted trends in each ensemble member and the ensemble-mean (e.g., forced) trend for (a) CMIP5 and (b) CESM1. Panel (c) shows the observed thermodynamic residual precipitation trend (note the different color bar compared to Fig. 1 in the main text). Stippled regions in (c) denote precipitation trends that are insignificant at the 90% confidence level based on a two-sided Student-t test. This comparison shows that the observed thermodynamic residual precipitation trend exceeds the error associated with the dynamical adjustment methodology at most locations.

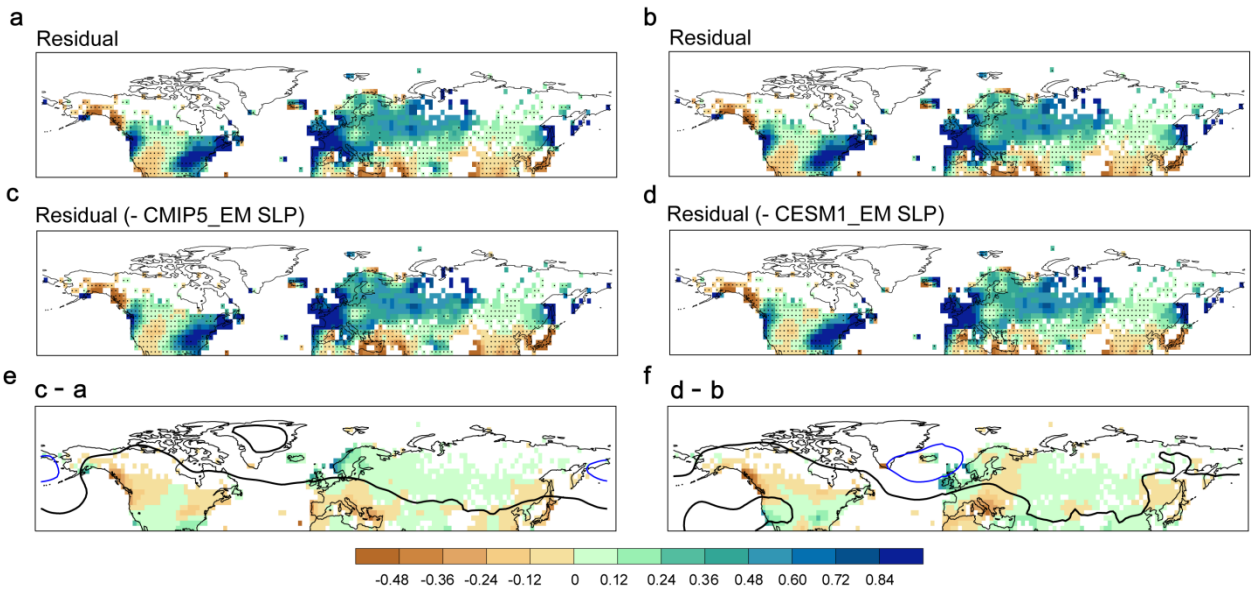

Figure S4. Sensitivity of the observed thermodynamic residual winter (November-March) precipitation trends (1921-2015; mm mo^{-1} per decade) to the forced component of SLP trends simulated by CMIP5 and CESM1. Panels (a) and (b) show the observed thermodynamic residual trends assuming no forced SLP trends. Panels (c) and (d) show the observed thermodynamic residual trends based on subtracting the CMIP5 and CESM1 ensemble-mean SLP trends, respectively, before applying the dynamical adjustment procedure. Contours show the ensemble-mean SLP trends at a contour interval of 0.1 hPa per decade (zero contour in black, and negative values in blue; there are no positive values). Stippled regions in a-d denote trends that are insignificant at the 90% confidence level based on a two-sided Student-t test. Panels (e) and (f) show the differences: (a) minus (c), and (b) minus (d). Note the different color bar compared to Fig. 1 in the main text.

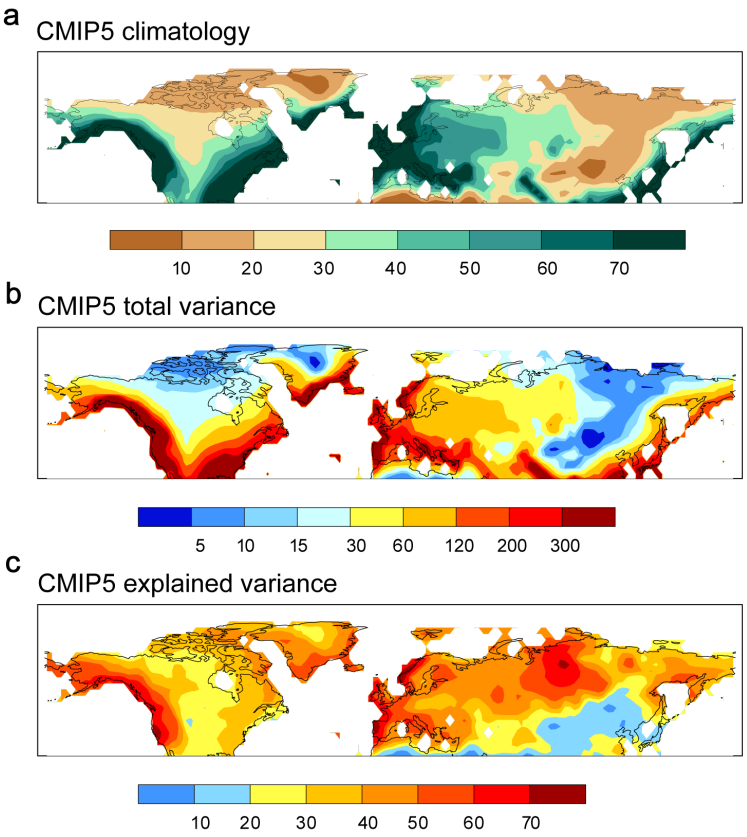

Figure S5. CMIP5 winter (November-March) precipitation (**a**) climatology (mm mo^{-1}), (**b**) interannual variance (mm $mo^{-1})^2$, and (**c**) percentage of interannual variance explained by dynamical adjustment (%) based on detrended data during 1921-2015, and averaged across all 37 models.

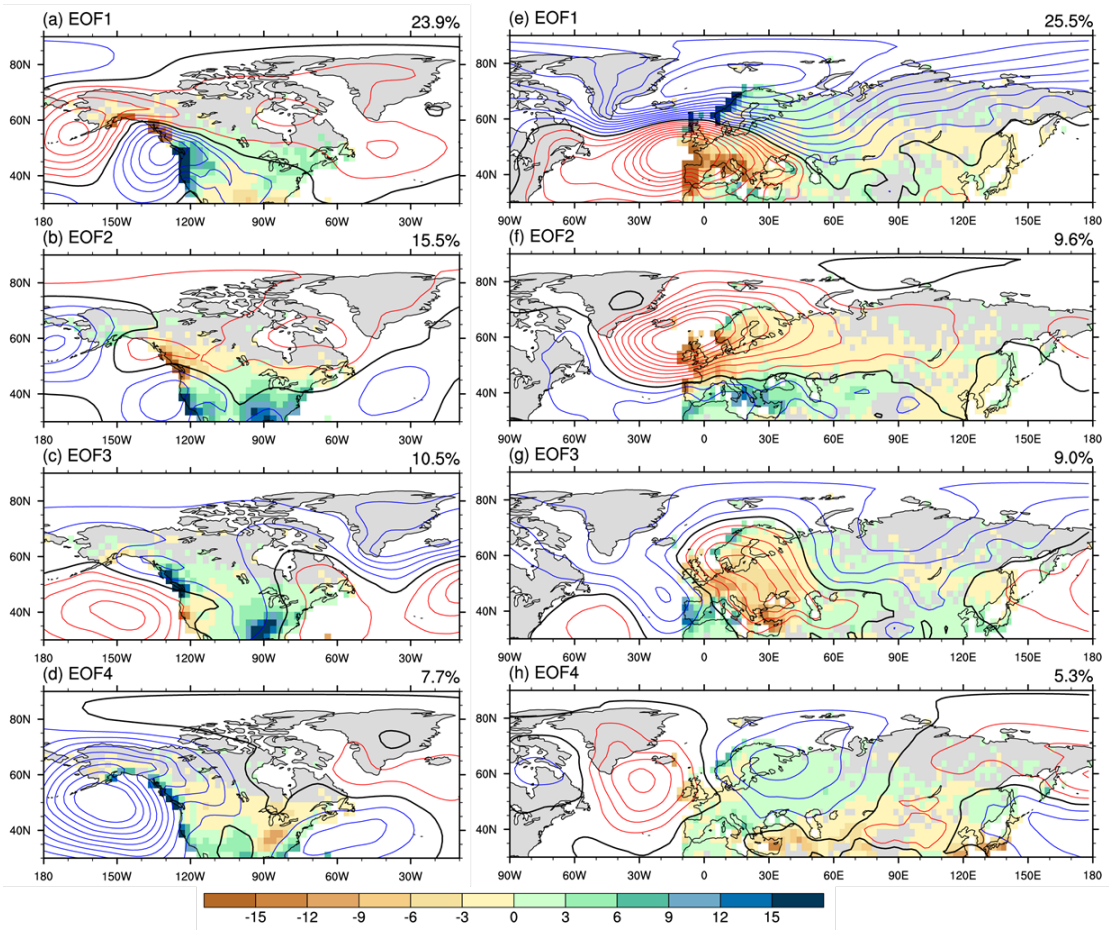

Figure S6. Regression maps of observed winter precipitation (color shading; mm mo^{-1}) and SLP (contour interval is 0.3 hPa, with positive (negative) values in red (blue) and the zero contour in black) anomalies upon the 4 leading normalized principal component time series of winter precipitation over (a-d) North America and (e-h) Eurasia, based on detrended data during 1921-2015. Values in the upper right corner denote the explained variance of each EOF. These results are indicative of a circulation-driven influence on interannual precipitation variability. For example, cyclonic (anticyclonic) circulation anomalies are associated with increased (diminished) rainfall in adjacent areas.

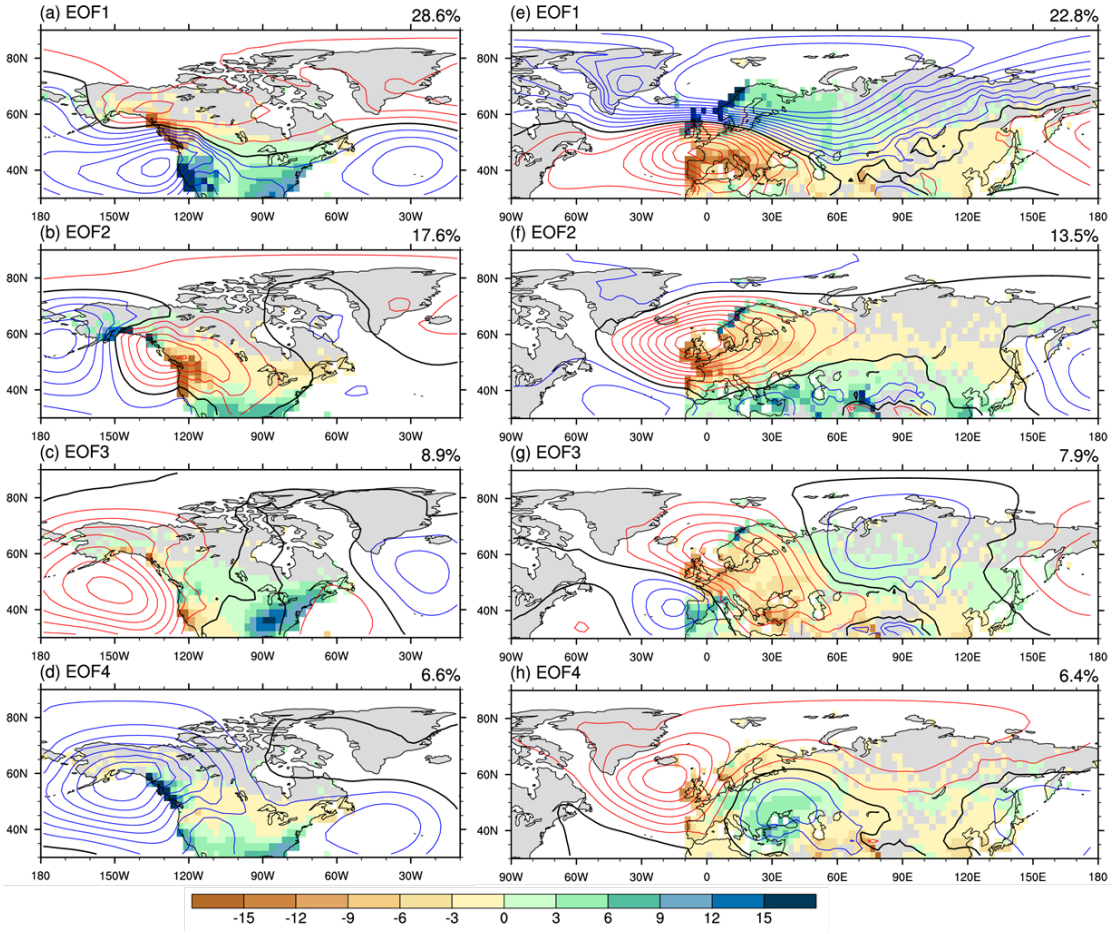

Figure S7. As in Fig. S6 but based on CESM1. The detrended data from each of the 40 ensemble members are appended together before computing the EOFs and associated principal component timeseries. CESM1 simulates realistic precipitation EOFs and associated SLP linkages (compare with observations in Fig. S6). Results for CMIP5 are similar (not shown).